Inlet Air Flow Sensing for the iSTC-21v Small Jet Engine

Róbert Czakó[1], Dávid Vaľko[2], Peter Gašparovič[1], Rudolf Andoga[3], Norbert Ádám[2], Ladislav Főző[1]

[1]Department of aeronautical engineering, Faculty of Aeronautics, Technical University of Košice, Rampová 7, 04001 Košice, Slovakia
robert.czako@student.tuke.sk, peter.gasparovic@tuke.sk, ladislav.fozo@tuke.sk

[2]Department of Computers and Informatics, Faculty of Electrical Engineering and Informatics, Technical University of Košice, Letná 9/A, 042 00 Košice, Slovakia
david.valko@tuke.sk, norbert.adam@tuke.sk

[3]Department of avionics, Faculty of Aeronautics, Technical University of Košice, Rampová 7, 04001 Košice, Slovakia
rudolf.andoga@tuke.sk

Abstract: Accurate measurement of the flow rate of air entering the jet engine is very important from the point of view of the design of control algorithms and diagnostic systems (e.g. when classifying situational frameworks of situational control, or when predicting unmeasured parameters or the failure of other measured parameters within the diagnostic system, the design and implementation of which for micro (JetCat P-80, TJ-20) and small (iSTC-21v, TJ-100) jet engines is devoted to the scientific research team of the Laboratory of Intelligent Aircraft Engines). In order to accurately measure the air flow rate in the entire cross-section of the inlet device of the iSTC-21v small jet engine based on the value of the local velocity, temperature and pressure, it is necessary to know the distribution of the absolute velocity at the entrance to the engine (e.g. we may be interested in the homogeneity of the absolute velocity and turbulence, by sensing which using CTA equipment or pressure probes, another scientific and research team of the Aerodynamic Tunnel Laboratory). The speed distribution is also influenced by the shape of the bell mouth – the leading edge of the newly designed iSTC-21v engine inlet assembly (as opposed to the classic engine inlet assembly, where the flow rate of air is not measured). Using the numerical CFD simulation in Ansys and the program for calculating the superellipse coordinates in Matlab, in the presented article we are devoted to the pilot design of the inlet device with the sensing of the air flow amount of the small jet engine iSTC-21v.

Keywords: jet engine inlet; iSTC-21v; air mass flow rate; CFD simulations; superellipse; bell mouth

1 Introduction

The research team of the Laboratory of Intelligent Aero Engines [1] (previously called the Laboratory of Intelligent Control Systems of Aircraft Engines) at the Aviation Faculty of the Technical University in Košice worked on a design and creation of mathematical models of complex nonlinear systems in jet engines for more than twenty years [2]. Problems involve the design, simulation and experimental verification of intelligent control [3], diagnostic systems of jet engines [4, 5] – micro and small – with the use of computational intelligence – neural networks, fuzzy systems, etc. The experience of the aforementioned laboratory is supplemented by skills of another unique workplace of the Aviation Faculty of the Technical University in Košice – the Aerodynamic Tunnels Laboratory [6] in the issue of the design of the new inlet device of the small jet engine iSTC-21v (see Fig. 1). There is also collaboration of these research teams in the ongoing national project entitled "Innovative measurement of airspeed of unconventional flying vehicles" [7], and collaboration with another faculty of the Technical University in Košice - Faculty of Electrical Engineering and Informatics (they were instrumental also during the creation and beginnings of the development of the Laboratory of Intelligent Aero Engines).

The design and later implementation of a new inlet device [8] with sensing of the air flow entering the small jet engine iSTC-21v (intelligent small turbocharger engine 21 with a variable outlet nozzle) necessitated another subtask, with participation of wide range of experts. Sensing the mass flow rate of air entering a jet engine is troublesome [9]. It is mostly performed only in laboratory [10] and production conditions, usually on the ground, and it is a very important parameter used in various calculations of unmeasured parameters obtained from the thermal cycle of aircraft engines. These parameters are used in the prediction of diagnostic systems as well as in the control system itself [11], specifically in the diagnostic-control-situational system of the small intelligent turbo-compressor engine iSTC-21v. So far, we have not solved the issue because it is difficult to change the design of the inlet device of jet engine iSTC-21v (see Fig. 1). In front of the jet engine compressor is electric starter ST-3PT. It is basically an electric motor, relatively large, powered by a DC voltage of 33 V and a current of 150 A, designed for short-term repetitive operation. During start-up, the rotor of the engine turbo-compressor is accelerated from zero rotational speed ($n=0$ min^{-1}) to its first stable mode ($n=18000$ min^{-1}) and then the starter automatically disconnects [3].

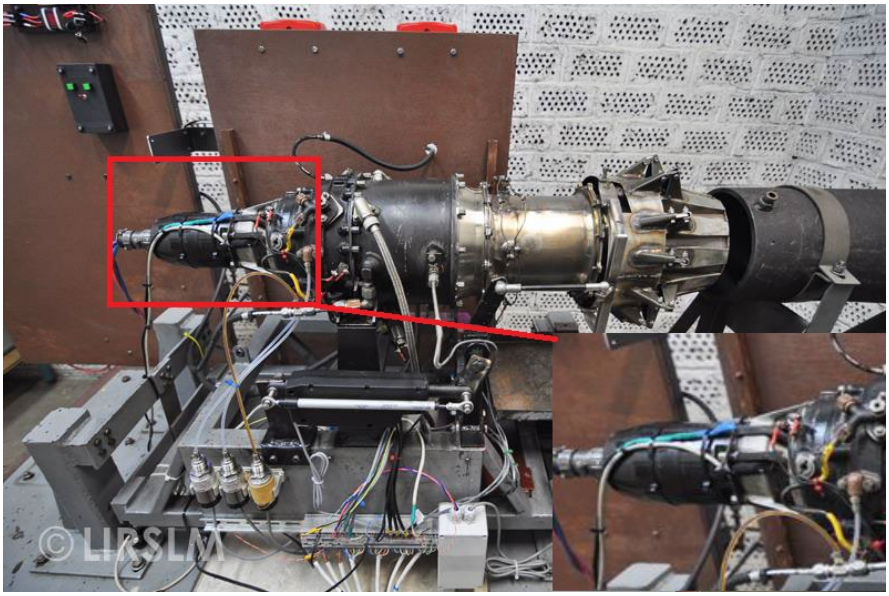

Figure 1
Intelligent small turbocharger engine iSTC-21 with a variable outlet nozzle (current inlet device is highlighted)

The insertion of current electric motor into inlet device with the form of extension tube (similar to that on Fig. 2) with narrow cross-section between the electric motor and inner surface of extension tube raises the question of sufficient air flow for the engine.

An alternative would be to replace the current electric motor fed from a strong stable source with a smart small electric motor built into compressor impeller of the iSTC-21v engine, or so that it is part of the engine structure and can be used to recharge the batteries after the engine starts up for independent operation. An example is a commercial modern small jet engine TJ-100 (see Fig. 2), which has an electric motor – with function of electric starter and generator – connected to batteries with direct current, max. current 120A. Such solution is portable and after initial start-up of the engine permits recharge of the batteries. It is smaller in size and the batteries also take up less space, are portable and easier to handle. In the case of iSTC-21v entire engine starting system would have to be designed, including the ignition coils and spark plugs, the fuel-oil pump and all aggregates used in engine starting, which is a big intervention into the entire jet engine starting and control system. For this reason, we proceeded to the design a new intake device with sensing of the mass flow of the air into the iSTC-21v engine with a current electric motor and to the investigation of its advantages and disadvantages, as we present it in the presented article. From the beginning, we focus on the measurement of the flow rate of incoming air through an extension tube, its mathematical expression and

verification according to the TJ-100 engine. Subsequently, in the next chapters, we deal with the specific design of a bell mouth - the leading edge of the inlet device and the sensing of the air flow rate of the iSTC-21v engine. In the end, the CFD simulations are used for evaluation of possible locations for the sensing of the pressure and velocity of the air in the inlet device. In the very conclusion, we mention the future plans and possible improvements – refinements for the design of the inlet device with the sensing of the flow of air to small engines in the Laboratory of Intelligent Aircraft Engines.

2 Sensing the Air Mass Flow Rate of a Jet Engine

The mass flow rate of air is measured according to the relation [12, 13]:

$$\dot{m} = \rho S v \tag{1}$$

where

ρ – is the air density [kgm^{-3}],

S – is the cross-sectional area [m^2], and

v – is the air speed [ms^{-1}].

In aviation practice, the knowledge of mass flow has several uses (besides the specific ones mentioned for laboratory conditions). From Newton's second law, we know that the normal aerodynamic forces acting on the surfaces are related to the change of momentum of the gas per unit time. Momentum is defined as the product of mass and velocity, which implies that aerodynamic forces are dependent on mass flow. The thrust of the drive unit is also dependent on the change of momentum of the working gas and thus is directly dependent on the mass flow rate. The mass flow is constant along the entire length of the tube [14, 15]. If we calculate (or choose) the exact value of the mass flow in any cross-section plane of this tube, we can calculate the mass flow in any other cross-section.

Measurement of air mass flow consist of two tasks – the measurement of air speed and the measurement of the air density. The measurement of air speed in whole cross-section is not practical, and we cannot measure air density directly. However, there are solutions to these problems. We start from the local pressure difference between atmosphere and inside of channel of the inlet device that arises due to the air flow. According to [9, 14], the entire derivation and the resulting equation for calculating the flow rate of air is as follows:

$$\dot{m} = \frac{p}{RT}\frac{\pi D^2}{4}\sqrt{\frac{2\Delta p}{\frac{p}{RT}}} \tag{2}$$

where

p – is the atmospheric pressure [Pa],

R – is the specific gas constant, for air R=287,1 [$JK^{-1}kg^{-1}$],

T – total temperature at the inlet to the inlet device [K],

D – diameter of the tube - inlet device [m], and

Δp – gauge pressure inside of inlet device [Pa].

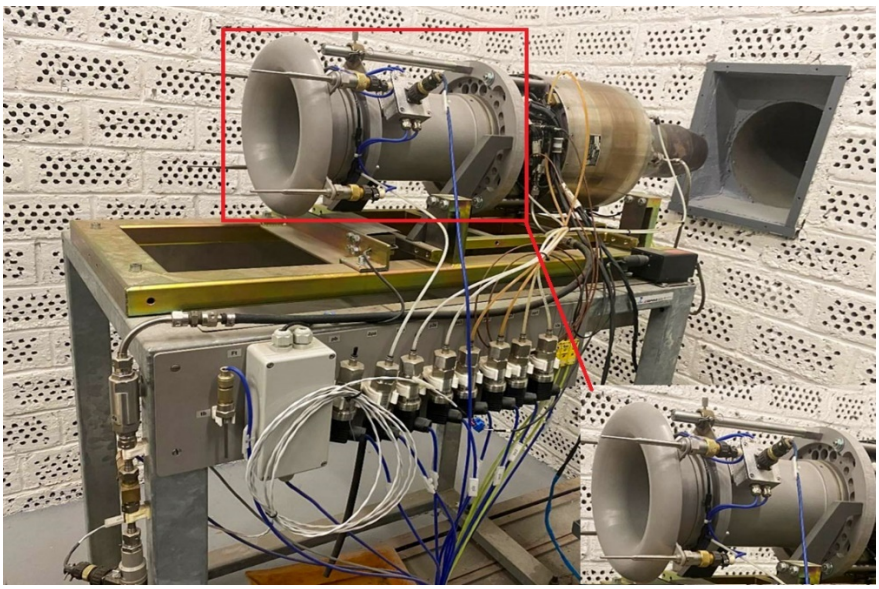

Figure 2
Small jet engine TJ-100 and its inlet device with air flow sensing

The correctness of the value according equation (2) was tested on a small jet engine TJ-100 (see Fig. 2), which is equipped with an inlet device for sensing the parameters of the air entering the engine, i.e. total temperature (t_{0c}), atmospheric pressure (pa) and gauge pressure in inlet (Δps). The equation value was compared with measured value in the LabView program as well as in Matlab and conclusion is that the calculation is correct. Another conclusion is that the mass flow rate of air is very little dependent on the outside temperature of the air - entering the engine inlet system.

3 Design of a New Inlet Device of Engine iSTC-21v

The development of the inlet device with the sensing of the air flow rate of the iSTC-21v engine was inspired by the commercial engine TJ100. Inlet consists of bell mouth and extension tube.

3.1 The Geometry of a Bell Mouth of Inlet Device

The inlet device must meet several conditions [8, 10]. The inlet device must have minimal pressure losses, the flow velocity at the inlet to the compressor must be homogenous, and there must be no separation of the air stream in the boundary layer.

Our highest priority is the design of the inlet device, the primary function of which is to provide the best possible conditions for measuring the temperature and pressure of the flowing air in order to calculate the mass flow rate of the air. One of the most important requirements is that there is are no vortices in the test section of inlet device. Vortices in the flow would significantly influence the measured values. According [10] the best design of the inlet device appears to be one in which the geometry of leading edge has bigger radius.

The limiting factors are dimensions and shape of the current iSTC-21v motor inlet device. We are limited also by the dimensions of the stand, the dimensions of the laboratory, and by the location of individual support systems and sensors around the engine. We must also take into account the availability of stock materials that will be used in production.

The design is based on the inlet geometry of the TJ-100 engine. The TJ-100 engine has similar dimensions as the iSTC-21v engine, so it served as a suitable reference for our design. Instead of direct computation of geometry based on required flow parameters we chose simpler method – starting with several geometries, and then analyzing whether the flow homogenity is within the relevant limits. In the present article, the analysis will be performed by CFD simulations, and in the future, experimental verification will be performed in the Wind Tunnel Laboratory.

The bell mouth geometry is traditionally described by a bell mouth because of its gradual decrease of curvature toward engine. According [10] also a superellipse is often used in the design of mouths of aircraft inlets. It is a curve that resembles an ellipse in shape, maintains geometric references between the main and minor axes, maintains symmetry with respect to these two axes, but has a slightly different curvatures compared to a regular ellipse.

$$\left|\frac{x}{a}\right|^{m} + \left|\frac{y}{b}\right|^{n} = 1 \tag{3}$$

The variables x and y in this case represent the coordinates in the Cartesian coordinate system. The variables a, b, m, n are positive numbers. For regular ellipse m and n equals 2.

Explicit equation (4) for y-coordinate:

$$y = b \cdot \sqrt[n]{1 - \left|\frac{x}{a}\right|^{m}} \tag{4}$$

The user has several options to influence the results:

- choose the ratio of the axes of the superellipse,
- choose the coefficients m, n and thereby influence the shape of the superellipse,
- choose scale.

As reference values, we used the dimensions of the TJ-100 engine inlet device, which will be used to calculate the coordinates of bell mouth. The leading edge has a height of 65 mm and a length of 30 mm. The obtained coordinates need to be imported into the CAD program, in which the 3D model of the proposed new iSTC-21v engine inlet device will be created (the STEP format was created and 3D models of individual parts of the iSTC-21v engine obtained by scanning were used).

3.2 Design of the Extension Tube of the Inlet Device

The assembly of the extension tube consists of a steel pipe with flanges on both ends. The front part contains ports for measuring static pressure. A special flange is fixed on the front part of the engine. At this stage, the design is preliminary. It is necessary to determine the exact dimensions of individual parts based on information about the stock products offered on the market.

In order to keep the flow as uniform as possible in the test section, it is necessary to have a constant internal cross-section of the extension tube along its entire length. We ignore length of the tube with an electric motor. The test section is in front of the electric motor, to avoid the risk of its interference on measure parameters of the air flow.

In the preliminary design of a tube, we mainly assume the use of stock products from the point of view of availability. Assuming the diameter of the landing surface on the electric starter holder 150.3 mm (see Fig. 1), the inner diameter of the tube must not be less than 151 mm. We limit the selection of stock tubes on products made of steel, plastic and aluminum. A huge number of pipes are available on the Slovak market, which differ in material, production process, service life and other properties. In the field of steel pipes, we will focus on precise seamless pipes. This type is produced by cold drawing and the output semi-finished product is rolled seamless pipes. Standard precision tubes are used in practically all areas of mechanical engineering. The pipes are made of carbon and alloy steels in the dimensions determined by the standard. For CFD analysis, we consider pipes with internal dimensions of 159 mm and 206 mm - they will provide us with sufficient information about how the state variables in the test section change with respect to the internal diameter of the tube.

In many areas of liquid distribution, we can meet plastic pipes today. Their main advantage is that they are not subject to corrosion and thus have a very long service life. However, this feature is of little importance to us, as the oven will not be

affected by the weather. Current plastic pipes are made from linear polyethylene (PE, PEHD, HDPE). PE pipes can be used to transport food, chemicals, compressed air and other gases. We can also use them to build pressure and vacuum sewers. In the case of aluminum products, there is no manufacturer of semi-finished products in Slovakia that would meet our requirements. For this reason, we will focus mainly on seamless steel pipes.

When designing the construction of the test section, we also have to deal with the issue of the length of the tube itself. Given that the maximum length of the electric starter is 236 mm, we will take this dimension as the limit. In addition to the electric starter, there will also be a cable that powers the electric starter in the measuring area. For this reason, we choose 400 mm as the shortest possible length of the tube of the test section. In order to know how the state variables in the test section depend on the length of the test section, we choose 500 mm and 600 mm as other possible lengths.

In order to be able to fasten the pipe to the electric starter holder, we need to find a suitable flange. In the case of the steel variant, the flange will be welded to the pipe with an overlap given by the relevant standard. We can find many different types of welding flanges on the market. For our use, the flat welding flange DN150 PN6 will be the most suitable (see Fig. 3).

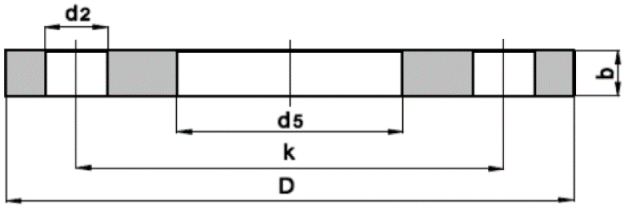

Figure 3
Flange DN150 PN6 [16]

The properties and dimensions of this flange are defined by the ČSN 131160 standard and can be found in Table 1.

Table 1
Flange dimensions DN150 PN6 [16]

pipe diameter	norm	D	d5	b	k	d4	f	Number of holes	d2
168,3	ČSN131160	265	169	20	225	202	3	8	18

To fix the measuring tube to the motor, we will need a custom-made flange with a different inner diameter. The seat surface of the electric starter has a diameter of 150.3 mm, so we choose the inner diameter d5 with regard to the tolerance of 151 mm. Other dimensions of the flange will be maintained as prescribed by ČSN 131160.

The most complicated part in terms of production is lemniskata – leading edge. This part cannot be purchased as a ready-made semi-finished product, but it must be made. The design of this part is based on the inlet system of the TJ-100 engine, from which we will take the length of the part – 30 mm. The flange joint will be based on the DN150 PN6 flange described in Table 1 and shown in Fig. 3. The shape of the leading edge will be based on the coordinates that we calculated using the Matlab script. In Fig. 4 we can see the visualization of the first prototype of the leading edge of the inlet system.

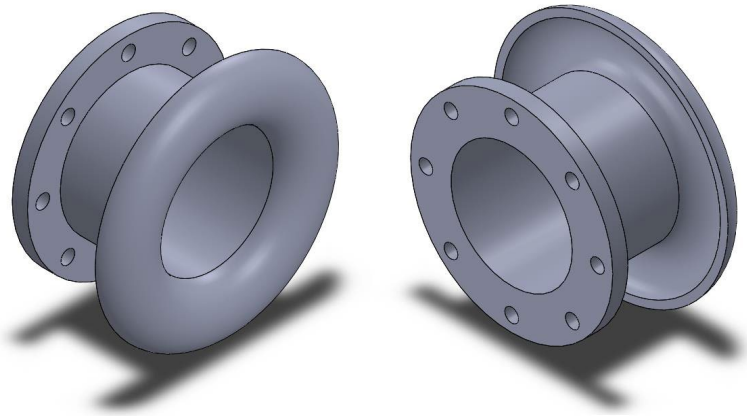

Figure 4
Visualization of the prototype leading edge of the inlet device

After modeling individual components in the environment of a 3D CAD program, it is possible to proceed to the assembly. The assembly of the first prototype will consist of the following parts:

- 1 piece – tailor-made flange according to ČSN 131160 with inner diameter d5 = 151 mm,
- 2 pieces – flange DN150 PN6 according to ČSN 131160,
- 1 piece - smooth seamless pipe PN6 with an inner diameter of 159 mm and a length of 400 mm,
- 1 piece – leading edge part with an inner diameter of 159 mm.

For CFD analyses, it will also be necessary to model the following parts:

- smooth seamless tube with an internal diameter of 159 mm and a length of 500 mm,
- smooth seamless tube with an internal diameter of 159 mm and a length of 600 mm,

- smooth seamless tube with an internal diameter of 206 mm and a length of 400 mm,
- smooth seamless tube with an internal diameter of 206 mm and a length of 500 mm,
- smooth seamless tube with an internal diameter of 206 mm and a length of 600 mm,
- flange flat welding DN200 PN6 according to ČSN 131160,
- tailor-made flat welding flange according to ČSN 131160 with inner diameter d5 = 151 mm,
- leading edge part with an internal diameter of 206 mm.

We chose these parts based on an analysis of the semi-finished product market and on the requirements for the design of the inlet device. By assembling the respective parts, we obtain a total of 6 different variants of the measuring area.

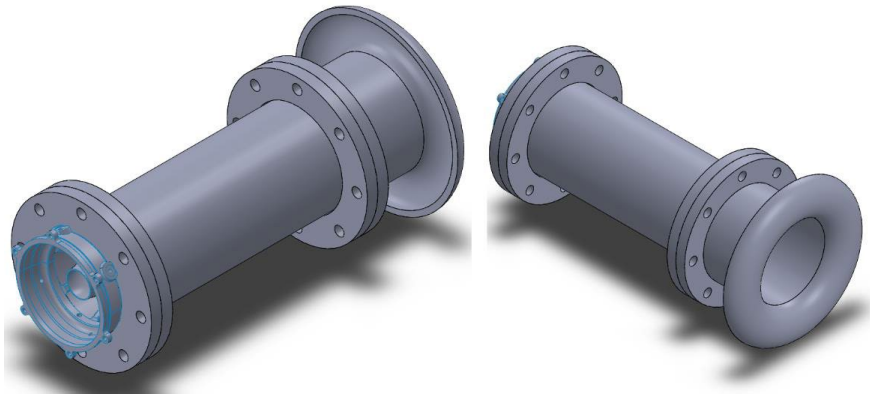

Figure 5
Visualization of the prototype measurement area assembly

Fig. 5 shows a visualization of the prototype assembly of the measuring area. This report will serve as the basis for creating the network needed for CFD analyses. No fasteners – that is, bolts, nuts and welds – have been implemented in the assembly. This design solution is not final and we will only take from it the geometry of the inner part, i.e. the inner part of the pipe, the leading edge, the shape of the electric motor and the shape of the inlet to the centrifugal compressor. The final design solution will be chosen based on the results of CFD analyses, but we will also take into account some other requirements, which we will familiarize ourselves with later.

4 CFD Analysis and Evaluation of Results

Before creating a network for CFD analysis, we need to simplify our design solution significantly. The following adjustments will be required:

- maintaining a constant internal cross-section in the tube (note: the internal cross-section changes around the electric starter, but we neglect this fact as we have significantly extended the test section),
- maintaining the shape of the leading edge (note: the outer shape of the leading edge is important, therefore, the inner part is completely filled; the termination is extended by 10 mm in order to reduce the number of low-quality elements),
- elimination of the gap that arises due to the prescribed overhang on the flange,
- simplification of the shape of the electric starter (note: we also neglect the power connector),
- simplification of the area at the inlet to the centrifugal compressor (note: the simplified area has the shape of a cone section),
- We neglect the outer part of the flange joints.

The result of these measures is a simplified geometry suitable for meshing. A comparison of the original and simplified geometry can be seen in Fig. 6(a) and Fig. 6(b).

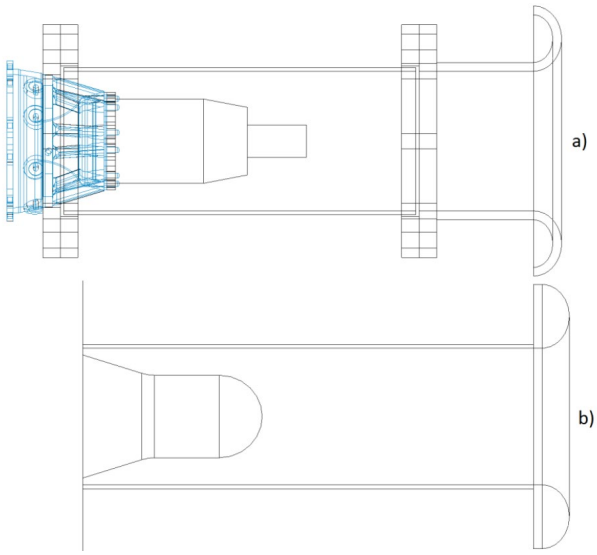

Figure 6
Comparison of original and simplified geometry

We then need to place the simplified geometry in an environment where airflow will be simulated. Our real environment is the room where the iSTC-21v engine is located. Since this room is very rugged, we simplify the surrounding environment to a simple cylinder. We chose a cylinder depth of 2000 mm and a radius of 2000 mm (see Fig. 7).

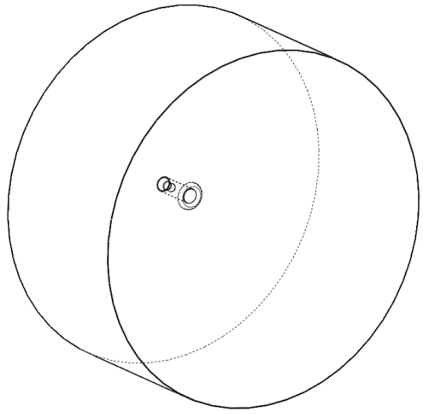

Figure 7
Outer CFD domain of inlet device

This process (note: modeling parts, assembling, simplifying geometry, modeling the environment) must be repeated for each desired prototype. The finished geometry is then converted to STEP format.

Correctly defining the network is a very complicated and lengthy process. Therefore, Ansys offers the possibility to generate the network automatically based on user-defined rules. This system will allow us to save time and create consistent rules for all networks that we will define. If a situation arises where the simulation fails due to a poorly generated network, we can easily adjust the network generation rules for all cases, saving time.

First of all, we need to check the quality of the geometry and establish tolerances. If we did not specify a tolerance, the netter could generate faulty nodes in the network. The next step is to merge some areas and name them. Fluent is already able to recognize some names, which can save us time when setting up the solver.

The next step consists in defining the rules for the network generator itself. First, we define an automatic method for the entire volume. Although we have the possibility to force tetrahedrones, we will not do so since in some places it will not be possible to generate tetrahedrones. These are mainly areas in the boundary layer. Another rule is the rule for generating elements in the boundary layer. We define this rule only for the respective areas – inner channel, leading edge and electric starter. We choose the number of layers 15. In the next step, we set the Face Sizing rule and chose 5 mm as the element size. We obtained this dimension experimentally. We repeat the procedure for each variant of the inlet device.

The generated network has from 1.4 to 2.1 million elements, depending on the design variant.

We chose Transition SST as the turbulence model. We did not use the energy equation in the simulation, as its impact was negligible. Air parameters have been predefined. As marginal conditions, we chose differential pressure that was equal to zero and its origin was located outside the simulated body. The output parameter was the mass air flow defined over the corresponding area. We changed its value based on our chosen requirements. Based on the technical manual for the small jet engine iSTC-21v (originally a turbo-starter), we created an assumption that the mass air flow will be m=1,3 kgs^{-1}. Thus, for each design variant we will simulate 4 Cases: for m=1 kgs^{-1}, for m=1,2 kgs^{-1}, for m=1,4 kgs^{-1} and for m=1,6 kgs^{-1}.

4.1 Evaluation of CFD Simulations

The result of each simulation is a graphical representation of the pressure field. Since it is a rotating body that is symmetrical according to plane XY (note: Cartesian coordinate system) for both variants, we will observe the pressure field in this plane. The total number of simulations performed is 24 and their results are shown in the graph in Fig. 8.

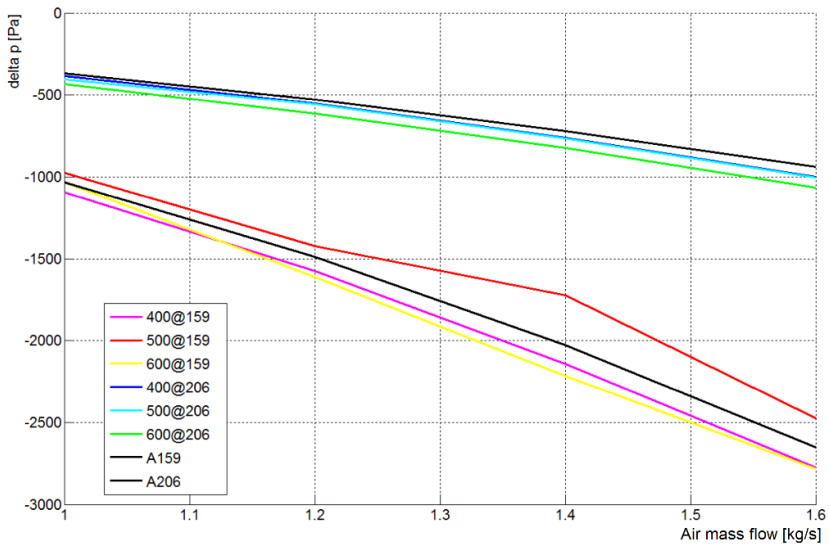

Figure 8
Comparison of analytical calculations and simulations

The differential pressure values in the Fluent program are not displayed exactly, but within a certain range. It follows that for a certain area in the test section a certain range of differential pressure values belong. In order to display these values in the graph, it was necessary to calculate the average pressure values in the areas of the

measuring area defined by us for each design variant. This is a time-consuming process during which results can be affected by human error, but also by the quality of the display device (e.g. monitor or projector). In this case, we had to focus on the area that is not affected by the electric starter and on the area that is not affected by the breakaway of the air flow at the end of the leading edge of the inlet system.

Based on the calculated average differential pressure values, we were able to plot these results in the graph in Fig. 8. This graph shows the dependence of mass air flow on differential pressure value for each design variant. Lines marked in black (NB. A159, A206) are the values obtained by analytical calculation. Several trends can be observed on the chart:

- with increasing value of mass air flow, the deviation of the simulated differential pressure and the calculated differential pressure increases,
- with increasing length of the test section, the deviation of the simulated differential pressure and the calculated differential pressure increases,
- with increasing internal cross-section of the test section, the deviation of the simulated differential pressure and the calculated differential pressure decreases.

Table 2

Comparison of variances of simulation and analytical calculations

L	m	MAE	MAPE	MAAE	L	m	MAE	MAPE	MAAE
400@159	1	59,5	5,75%	74,5	400@	1	17	4,63%	25,5
400@159	1,2	83,9	5,63%	98,9	400@	1,2	22,3	4,21%	34,8
400@159	1,4	115,5	5,69%	130,5	400@	1,4	40,2	5,58%	56,7
400@159	1,6	124,2	4,69%	139,2	400@	1,6	60,7	6,45%	82,2
500@	1	75	7,24%	135,5	500@	1	37,5	4,63%	52,5
500@	1,2	75	5,03%	141,1	500@	1,2	25,8	4,88%	40,8
500@	1,4	304,5	15%	379,5	500@	1,4	44,7	6,21%	59,7
500@	1,6	175,8	6.63%	250,8	500@	1,6	64,2	6,82%	79,2
600@	1	15	1,45%	15,5	600@	1	67,5	18,4%	82,5
600@	1,2	122,4	8,21%	172,9	600@	1,2	85,8	16,2%	100,8
600@	1,4	188,5	9,29%	238,5	600@	1,4	104,7	14,5%	119,7
600@	1,6	135,2	5,1%	211,2	600@	1,6	124,2	13,2%	139,2

In Table 2 we can find a comparison of differential pressure deviations obtained by simulation and analytical calculation of individual design variants. Variants whose simulation and analytical calculation variations are too large or not consistent are indicated in red. Variants with a measuring tube length of 600 mm have the highest deviations from analytical calculations, while variants with a tube length of 400 mm have the smallest. The tolerances for variants with a tube length of 400 mm and an inner diameter of 159 mm and 206 mm and a variant with a tube length of 500 mm and an inner diameter of 206 mm appear to be the most suitable for our application.

The Fluent program displays differential pressure values in a certain range. This range refers to a certain volume in our body. This elementary volume has the shape of a cylinder, the content of which depends on the inner diameter of the test section. The height of the cylinder in this case is chosen manually on the basis of the conditions defined in the introduction to this subchapter. Since it is a rotationally symmetrical body, we read the differential pressure from the section that passes through plane XY, which is also the plane of symmetry. Thus, the elementary cylinder was reduced to a rectangle. This elementary rectangle will represent the section in which it is most convenient to place the pressure sensing ports. Since the construction variants with a measuring tube length of 400 mm and internal diameters of 159 mm and 206 mm show the best results, we will continue to work only with them.

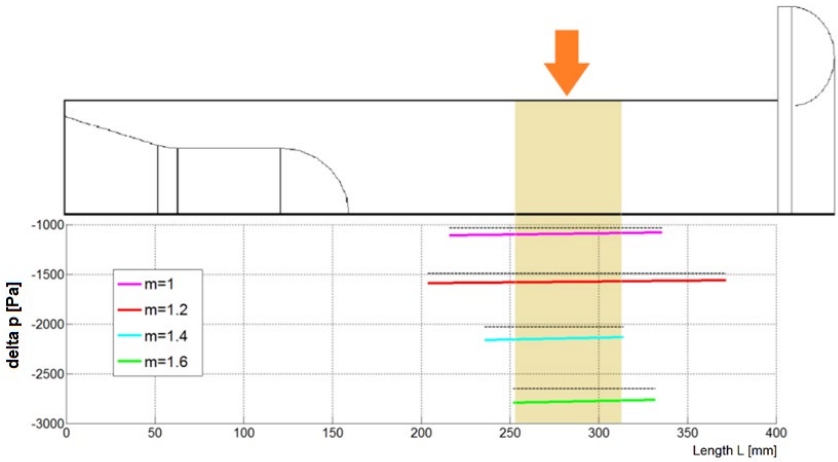

Figure 9

Graphical display of the most suitable sensor placement (D = 159 mm)

In the graph in Figs. 9 and 10, we can see the sections that we subtracted from the Fluent program. The lengths and location of the sections in relation to the length of the measuring tube are indicated in colour (pink, red, turquoise, green). There is differential pressure on the Y axis and it is only informational in nature. The light brown color indicates the area that is the intersection of the individual lengths of the elementary sections. Above the graph there is a graphical representation of this area directly on the drawing of the inlet device structure. We will consider this section as the final solution.

The elementary section starts at a distance of approximately 252 mm from the compressor inlet and has a length of approximately 62 mm and 84 mm respectively. These values are not exact, as we have to take into account inaccuracies when reading data from the Fluent program. The orange arrow in Figs. 9 and 10 indicate the expected location of the pressure sensing ports.

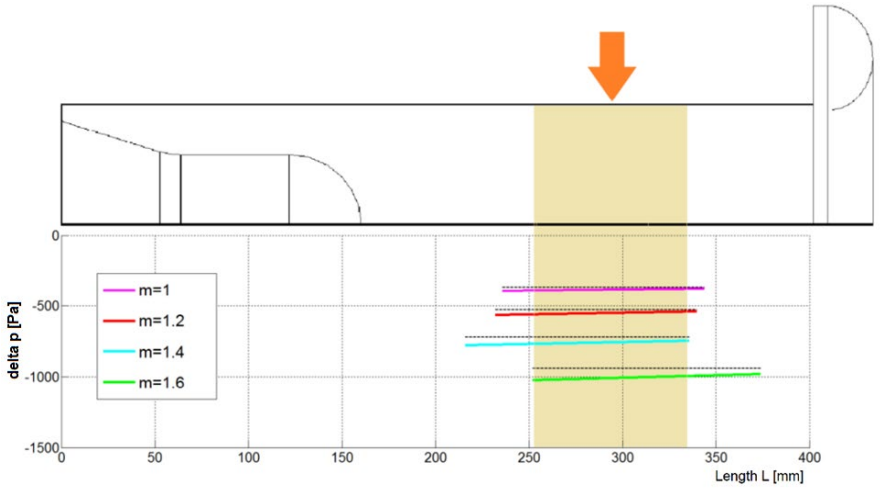

Figure 10
Graphical display of the most suitable sensor placement (D = 206 mm)

4.2 Continuation of Inlet Device Development

Based on existing knowledge, it is possible to manufacture the inlet device designed by us and verify its functionality by experiment. The first step after the completion of the development phase is to generate the relevant drawings, which will serve as the basis for the production itself, but also for the valuation of the parts proposed by us. The most complex component of our designed inlet device is the leading edge. This part is quite complicated, mainly because it is necessary to maintain maximum accuracy of the leading-edge profile. The inaccuracies could then be reflected in the results of differential pressure measurements in the measuring area. These inaccuracies could arise precisely during production, both due to the incorrectly chosen production technology, but also to the experience of the worker who would be machining this product. Since it is a complicated part, it will be necessary to use a combination of several production technologies – turning, milling and drilling. For this reason, it would be very convenient to return to the development phase and reconsider some design solutions.

For CFD analyses, it was necessary to significantly simplify our proposed assembly of parts so that it could be used for network generation. These CFD analyses were thus simulated for this simplified variant of the test section. This knowledge allows us to rethink the current design solution. The internal profile of the test section will serve as a basis. The condition for the new design is, therefore, to maintain the same internal profile of the test section. The new structural design can be seen in Fig. 11.

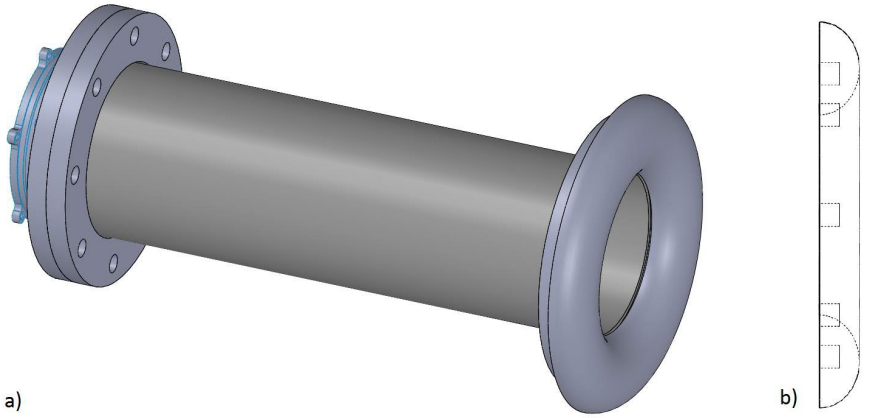

Figure 11
Alternative design of the inlet device

The new structural design includes several advantages, but also several disadvantages. The new design succeeded in maintaining the same internal profile of the inlet device, as this was the main and most important requirement. The mouth part has been simplified so that it can be produced with one tool per cycle. The new profile of this part can be seen in Fig. 11 (b). The demand placed on the production of this part are very high, as it is the most important part of the entire project. The quality of this part will directly affect the measurements in this inlet device. We must also take into account that this leading-edge profile is only the first draft that serves as a basis for further research. In the previous chapters, we got acquainted with the fact that the development of the inlet device is experimental. Despite the fact that we have precise software simulation tools such as Ansys Fluent, the final design solution must be verified experimentally on the actual inlet device. This fact had to be taken into account when creating a new design solution, as this can significantly reduce the financial costs of leading-edge production, but also save time. Another important factor is that we can also make such a simple part from other materials, but also using other production technologies.

The leading edge in our case does not transfer any structural loads, thereby significantly expanding the range of usable materials. An example would be the use of 3D printing. In this case, however, more emphasis would have to be placed on surface treatment, which could ultimately have a negative impact on the flow around the leading edge. To compensate for the shortening of the mouth part, it was necessary to extend the inlet tube itself so that the original internal profile of the test section was maintained.

Conclusions

In the present article, two scientific research teams of the Intelligent Aero Engines Laboratory and the Wind Tunnel Laboratory of the Faculty of Aeronautics and the

Faculty of Electrical Engineering and Informatics of the Technical University in Košice implemented a pilot design of a new inlet system with air flow sensing of the iSTC-21v engine. The advantage of the whole proposal is flexibility in terms of further development. In the relevant chapters, we have determined that the most optimal inlet variant must be as short as possible. We have also determined the range of internal diameters of the inlet system, allowing for greater flexibility with regard to the tubular semi-finished product used. The leading-edge profile can be designed quickly and easily in the appropriate script for calculating profile coordinates. The advantage of this solution is that the user is not tied to one specific CAD program, but can choose the program of his choice. The use of semi-finished products such as seamless pipes and flanges is convenient in terms of financial and time, and at the same time allows the manufacturer to choose at its discretion.

Standard aircraft engine inlets do not use air flow sensing, but it is very important in laboratory conditions. Especially in the area of design and efficiency of modern and intelligent control and diagnostic systems of complex systems [17, 18, 19]. In the future, we will improve the pilot design of sensing the flow amount of air and the bell mouth itself – the leading edge of the inlet system based on the above-mentioned CTA - Constant Temperature Anemometry method and measurements and achieve more precise sensing of the distribution of air flow at the inlet of a small jet engine.

Acknowledgement

This work was supported by the Slovak Research and Development Agency under the number APVV-20-0546 – "Innovative measurement of airspeed of unconventional flying vehicles" and VEGA, Grant Agency of Ministry of Education and Academy Science of Slovak Republic under Grant No. 1/0701/23 – "Efficient control algorithms of small aircraft turbo-compressor engines." The work was support of research and development potential in the area of transport means with ITMS project code: 313011T557. This support is very gratefully acknowledged.

References

[1] L. Főző, "Description of an intelligent small turbocompressor engine with variable exhaust nozzle," SAMI 2015 - Danvers : IEEE, 2015 S. 157-160 - ISBN 978-1-4799-8220-2

[2] G. G. Kulikov, A. Thompson, "Dynamic Modelling of Gas Turbines Identification, Simulation, Condition Monitoring and Optimal Control," Springer, 2004, p. 337

[3] R. Hanz**,** "Advanced Control of Turbofan Engines," Springer, 2012, p. 225, L. Főző, "Description of an intelligent small turbocompressor engine with variable exhaust nozzle," SAMI 2015 - Danvers : IEEE, 2015 S. 157-160 - ISBN 978-1-4799-8220-2

[4] G. Sanjay, “Controls and Health Management Technologies for Intelligent Aerospace Propulsion Systems,” Glenn Research Center, AIAA–2004–0949, NASA/TM—2004-212915

[5] J. Csank et al., “Control Design for a Generic Commercial Aircraft Engine,” Glenn Research Center, AIAA–2010–6629, NASA/TM—2010-216811

[6] P. Gašparovič, et al., “Improvement of wind tunnel flow with screens,” New Trends in Aviation Development 2019 - Danvers (USA) : Institute of Electrical and Electronics Engineers pp. 64-67, ISBN 978-1-7281-4078-0

[7] P. Gašparovič, et al., “Project IMAF – research on measurement of airspeed of unconventional flying vehicles,” Acta Avionica, Vol. 23, Is. 2, 2021, pp. 21-24, ISSN 1335-9479

[8] J. Seddon, E. L. Goldsmith, “Intake Aerodynamics,” American Institute of Aeronautics and Astronautics, p. 407, 1999, ISBN:9781563473616

[9] S. Wehofer ARO, Inc. and. R. Rivir, “Measurement of Turbine Engine Transient Airflow in Ground Test Facilities,” Aero-Propulsion Laboratory, Wright-Patterson Air Force Base, Ohio, p. 77, 1980

[10] R. W. Luidens, N. O. Stockman, J. H. Diedrich, “An approach to optimum subsonic inlet design, “ Cleaveland, Ohio, ASME, 1979

[11] Zs. Faltin, K. Beneda, “Establishment of Meanline Compressor Mathematical Model with Active Blade load Distribution Control,” 2020 IEEE 18th World Symposium on Applied Machine Intelligence and Informatics (SAMI), pp. 23-25, DOI:10.1109/SAMI48414.2020.9108751

[12] F. Whittle, “Gas Turbine Aero-Thermodynamics With Special Reference to Aircraft Propulsion,“ 1483293211, p. 276, Elsevier Science, 2013, ISBN 9781483293219

[13] P. Vírostek, “Design of an airflow measurement system on a small turbojet engine“, Technical university of Kosice, 2017

[14] P. Patrício, J. M. Tavares, A. J. Phys, **“**Simple thermodynamics of jet engines,“ 2010, 78 (8), pp. 809-814

[15] R. D. Flack, “Fundamentals of Jet Propulsion with Applications,“ Cambridge U. P., New York, 2005

[16] Armatury Group a.s., Nádražní 129, 742 22 Dolní Benešov (2009) Flanges, products – catalogue, link: https://www.armaturygroup.cz/ke-stazeni/_dc6

[17] C. Pozna, R. E. Precup, “On the Use of Quaternions, in the Translated Reference Frame Formalism,“ Acta Polytechnica Hungarica, Vol. 20, No. 6, 2023, ISSN 1785-8860

[18] G. Györök, B. Beszedes, “Adaptive Optocoupler Degradation Compensation in Isolated Feedback Loops,” 2018 IEEE 12th International Symposium on

Applied Computational Intelligence and Informatics (SACI), Timisoara, Romania, 2018, pp. 000167-000172

[19] J. K. Tar, J. F. Bitó, I. J. Rudas, "Contradiction Resolution in the Adaptive Control of Underactuated Mechanical Systems Evading the Framework of Optimal Controllers," Acta Polytechnica Hungarica, Vol. 13, No. 1, 2016, ISSN 1785-8860